

# $^{17}\text{O}$ Magic Angle Spinning NMR Studies of Brønsted Acid Sites in Zeolites HY and HZSM-5

Luming Peng,<sup>†</sup> Hua Huo,<sup>†</sup> Yun Liu,<sup>‡</sup> and Clare P. Grey<sup>\*,†</sup>

Contribution from the Department of Chemistry, State University of New York at Stony Brook, Stony Brook, New York 11794-3400, and Institute of Geochemistry, Chinese Academy of Sciences, 46 Guanshui Road, Guiyang, Guizhou 550002, P. R. China

Received July 11, 2006; E-mail: cgrey@notes.cc.sunysb.edu

**Abstract:** High-resolution  $^{17}\text{O}/^1\text{H}$  double resonance NMR spectra were obtained for two zeolites, one with a low Si/Al ratio (zeolite HY) and one with a high Si/Al ratio (HZSM-5), to investigate their local structure and Brønsted acidity. Two different oxygen signals, corresponding to Brønsted acid sites in supercages and sodalite cages of zeolite HY were readily resolved in the two-dimensional (2-D)  $^1\text{H}$ - $^{17}\text{O}$  heteronuclear correlation (HETCOR) NMR spectra allowing the  $^{17}\text{O}$  isotropic chemical shift ( $\delta_{\text{CS}}$ ) and quadrupolar coupling parameters (quadrupolar coupling constant, QCC, and asymmetry parameter,  $\eta$ ) for the two oxygen atoms to be extracted. Similar experiments for HZSM-5 showed that the sites in this system are associated with a much larger distribution in NMR parameters than found in HY.  $^{17}\text{O}$ - $^1\text{H}$  rotational echo double resonance (REDOR) NMR was applied to probe the O-H distances in zeolites HY and HZSM-5. Weaker  $^{17}\text{O}$ - $^1\text{H}$  dephasing was observed for zeolite HZSM-5 in comparison to that of HY, consistent with longer O-H bonds and/or increased proton mobility.

## Introduction

Zeolites continue to attract considerable attention,<sup>1-3</sup> since these microporous aluminosilicates have widespread industrial applications, especially in catalysis and separations and more recently in medical applications. The unique porous structures of zeolites, along with their acidity, play a vital role in controlling the activity and selectivity of many zeolite-based catalysts.<sup>4,5</sup> Solid-state NMR spectroscopy represents a very powerful tool with which to investigate the local structure of solids.  $^{29}\text{Si}$ ,  $^{27}\text{Al}$ , and  $^1\text{H}$  NMR spectroscopies are standard analytical tools in studies of zeolites and have been widely used to probe acidity and to quantify the number of different crystallographic sites, silicon to aluminum  $n(\text{Si})/n(\text{Al})$  ratio and coordination numbers of the aluminum species.<sup>6,7</sup> The only NMR active oxygen isotope,  $^{17}\text{O}$ , is a quadrupolar nucleus ( $I = 5/2$ ), thus, both the chemical shift and electric field gradient (EFG) can be exploited to investigate local environments.  $^{17}\text{O}$  has a very large chemical shift range ( $>1000$  ppm) and the EFG tensor at oxygen nucleus is directly related to the charge

distribution at the oxygen atoms and the nearby atoms/ions.<sup>6,8-10</sup> Furthermore, the oxygen atom has the largest ionic radius of the typical atoms in the zeolite structure; hence, it is expected to be intimately involved in adsorption and catalytic processes.<sup>11</sup> Therefore,  $^{17}\text{O}$  NMR spectra should, in principle, yield considerable information.<sup>12</sup> However,  $^{17}\text{O}$  NMR investigations of zeolites are still not routine, largely because of the relatively low resonant frequency of  $^{17}\text{O}$ , its very low natural abundance (0.037%), and thus the need to enrich the samples, and its relatively large  $^{17}\text{O}$  quadrupole moment. The latter often broadens the  $^{17}\text{O}$  NMR signals making them very difficult to observe and interpret.

With the developments in high magnetic field strengths and fast magic angle spinning (MAS) NMR techniques, high resolution  $^{17}\text{O}$  NMR spectra have been collected for a variety of zeolites, such as zeolite A,<sup>13-15</sup> X,<sup>14,16</sup> Y,<sup>17</sup> and ZSM-5.<sup>14,18</sup>

<sup>†</sup> State University of New York at Stony Brook.

<sup>‡</sup> Chinese Academy of Sciences.

- (1) Corma, A.; Rey, F.; Rius, J.; Sabater, M. J.; Valencia, S. *Nature* **2004**, *431*, 287-290.
- (2) Greaves, G. N.; Meneau, F.; Majerus, O.; Jones, D. G.; Taylor, J. *Science* **2005**, *308*, 1299-1302.
- (3) Paillaud, J. L.; Harbuzaru, B.; Patarin, J.; Bats, N. *Science* **2004**, *304*, 990-992.
- (4) Corma, A. *Chem. Rev.* **1995**, *95*, 559-614.
- (5) Karge, H. G.; Hunger, M.; Beyer, H. K. In *Catalysis and Zeolites: Fundamentals and Applications*; Weitkamp, J., Puppe, L., Eds.; Springer: New York, 1999; 198-326.
- (6) Grey, C. P. In *Handbook of Zeolite Science and Technology*; Auerbach, S. M., Carrado, K. A., Dutta, P. K., Eds.; Marcel Dekker: New York, 2003; 205-255.
- (7) Klinowski, J. *Anal. Chim. Acta.* **1993**, *283*, 929-965.
- (8) Mueller, K. T.; Wu, Y.; Chmelka, B. F.; Stebbins, J.; Pines, A. *J. Am. Chem. Soc.* **1991**, *113*, 32-38.
- (9) Bull, L. M.; Cheetham, A. K. *Stud. Surf. Sci. Catal.* **1997**, *105*, 471-477.
- (10) Grandinetti, P. J.; Baltisberger, J. H.; Farnan, I.; Stebbins, J. F.; Werner, U.; Pines, A. *J. Phys. Chem.* **1995**, *99*, 12341-12348.
- (11) Bull, L. M.; Bussemer, B.; Anupold, T.; Reinhold, A.; Samoson, A.; Sauer, J.; Cheetham, A. K.; Dupree, R. *J. Am. Chem. Soc.* **2000**, *122*, 4948-4958.
- (12) Profeta, M.; Mauri, F.; Pickard, C. J. *J. Am. Chem. Soc.* **2003**, *125*, 541-548.
- (13) Pfeifer, H.; Freude, D.; Hunger, M. *Zeolites* **1985**, *5*, 274-286.
- (14) Pingel, U. T.; Amoureux, J. P.; Anupold, T.; Bauer, F.; Ernst, H.; Fernandez, C.; Freude, D.; Samoson, A. *Chem. Phys. Lett.* **1998**, *294*, 345-350.
- (15) Readman, J. E.; Kim, N.; Ziliox, M.; Grey, C. P. *Chem. Commun.* **2002**, 2808-2809.
- (16) Freude, D.; Loeser, T.; Michel, D.; Pingel, U.; Prochnow, D. *Solid State Nucl. Magn. Reson.* **2001**, *20*, 46-60.
- (17) Bull, L. M.; Cheetham, A. K.; Anupold, T.; Reinhold, A.; Samoson, A.; Sauer, J.; Bussemer, B.; Lee, Y.; Gann, S.; Shore, J.; Pines, A.; Dupree, R. *J. Am. Chem. Soc.* **1998**, *120*, 3510-3511.
- (18) Amoureux, J. P.; Bauer, F.; Ernst, H.; Fernandez, C.; Freude, D.; Michel, D.; Pingel, U. T. *Chem. Phys. Lett.* **1998**, *285*, 10-14.

The  $^{17}\text{O}$  signals from Si–O–Al and Si–O–Si linkages have been resolved and characterized in this prior work; however, the signal from the most catalytically relevant oxygen atoms, the ones that are directly bound to Brønsted acid sites, were not detected. Some of the difficulties associated with observing these sites arise from their large (predicted) quadrupole coupling constants,<sup>19,20</sup> their low concentrations, particularly in zeolites with high Si/Al ratios, the need to study dehydrated samples, and the need to devise new methods for enriching the samples in  $^{17}\text{O}$ . Zeolite samples are typically enriched by heating in  $\text{H}_2^{17}\text{O}$  or  $^{17}\text{O}_2$  at elevated temperatures. Generally, a temperature of 200–450 °C<sup>14,16,18,21,22</sup> was used for enrichment involving  $\text{H}_2^{17}\text{O}$  (although enrichment at only 95 and 125 °C was reported in two papers),<sup>9,23</sup> while a higher temperature of 550–750 °C<sup>9,11,15,17</sup> was applied if using  $^{17}\text{O}_2$ . Both methods lead to significant dealumination of acidic zeolites, as has been clearly documented in earlier literature.<sup>24,25</sup> Thus, in our earlier study of HY,<sup>26</sup> we solved this problem by first synthesizing  $^{17}\text{O}$ -enriched NaY, which is stable at elevated temperatures. NaY was then converted to  $\text{NH}_4\text{Y}$  via an ion-exchange reaction, which was then heat treated to produce dehydrated, enriched HY. We then used high magnetic fields and one-dimensional (1-D)  $^{17}\text{O}$  MAS double resonance NMR techniques to detect this elusive signal for the first time.<sup>26</sup> We now demonstrate that similar methods may be used to study a zeolite with a much higher  $n(\text{Si})/n(\text{Al})$  ratio (HZSM-5 ( $n(\text{Si})/n(\text{Al})$  ratio of 25) and report a more detailed investigation of the lower  $n(\text{Si})/n(\text{Al})$  ratio zeolite HY ( $n(\text{Si})/n(\text{Al})$  ratio of 2.6); both these zeolites are widely used as acid catalysts. We apply the 1-D and two-dimensional (2-D)  $^{17}\text{O}/^1\text{H}$  double resonance techniques, such as  $^1\text{H} \rightarrow ^{17}\text{O}$  cross-polarization (CP) NMR and  $^{17}\text{O}$ - $^1\text{H}$  rotational echo double resonance (REDOR) NMR, and demonstrate that, by making use of these double resonance experiments, Brønsted acid sites can be detected even if they are not directly visible in the simple one-pulse experiments. The zeolites contain Brønsted acid sites in different cages and channels (Figure 1) and we use  $^1\text{H}$ - $^{17}\text{O}$  heteronuclear correlation (HETCOR) NMR to resolve these different sites. The use of REDOR and variable temperature experiments for probing O–H distances and proton mobility are explored.

## Experimental Section

**Materials Preparation.** NaZSM-5 was prepared from  $\text{NH}_4\text{ZSM-5}$  ( $n(\text{Si})/n(\text{Al})$  ratio of 25; Zeolyst) by ion exchange (repeated three times) with a 1 M  $\text{NaNO}_3$  solution. The slurry was held at room temperature for 12 h, whereupon the solid was filtered, washed with distilled water, and then dried at ambient temperature. The resulting NaZSM-5 and NaY (Strem Chemicals) samples were enriched as described previously,<sup>15</sup> by heating a dehydrated sample in  $^{17}\text{O}_2$  gas (59.6% enriched  $^{17}\text{O}_2$ ; Isotec, Inc.) at 853 K for 12 h.  $^{17}\text{O}$ -enriched zeolite  $\text{NH}_4\text{Y}$  was

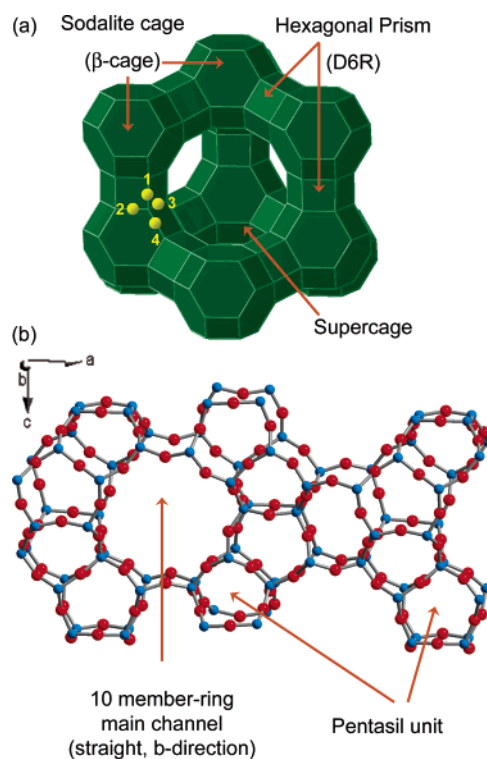


**Figure 1.** Structures of (a) HY and (b) HZSM-5. The Brønsted acid sites have been located, by using diffraction methods, in both the super- and sodalite cages of HY<sup>27</sup> and are believed, on the basis of semiempirical quantum calculations, to be located in both the channels and inside the pentasil units in HZSM-5.<sup>28</sup>

prepared by ion exchange with a 1 M  $\text{NH}_4\text{NO}_3$  solution at ambient temperature for 12 h (repeated five times).  $^{17}\text{O}$ -enriched  $\text{NH}_4\text{ZSM-5}$  was prepared by ion exchange with a 1 M  $\text{NH}_4\text{NO}_3$  solution at 353 K for 12 h (repeated three times). In order to obtain zeolites HY and HZSM-5,  $^{17}\text{O}$ -enriched  $\text{NH}_4$ -form zeolites were slowly heated from room temperature to 383 K in 7 h, and then to 673 K in 12 h where the temperature was held at 673 K for a further 12 h. All the samples were kept and packed in the  $\text{N}_2$  glove box prior to the NMR experiments.

**Solid-State NMR Spectroscopy.** MAS NMR spectra were obtained with Varian Infinityplus 500, Bruker Avance 600 and 750 spectrometers, with 89 mm wide-bore 11.7, 14.1, and 17.6 T superconducting magnets, in 4 mm rotors at 67.8, 81.4, and 101.7 MHz, respectively. Rotor caps with o-rings were used to avoid the adsorption of water during the NMR measurements.  $^{17}\text{O}$  and  $^1\text{H}$  chemical shifts are referenced to  $\text{H}_2\text{O}$  and  $\text{CHCl}_3$  (0.0 and 7.26 ppm, respectively). The Hartmann–Hahn condition for the CP and 2-D HETCOR NMR experiments was set by using the  $^{17}\text{O}$ -enriched zeolite HY sample. The NMR pulse sequences are shown in Figure 2. NMR line shape simulations were performed with the Wsolids package developed by Dr. K. Eichele or the SIMPSON package developed by Dr. N. Nielsen and co-workers.<sup>29</sup>

## Results and Discussion

**One-Pulse  $^{17}\text{O}$  MAS NMR.** The one-pulse  $^{17}\text{O}$  MAS NMR spectra of zeolite HZSM-5 ( $n(\text{Si})/n(\text{Al})$  ratio of 25), at various external magnetic fields, are shown in Figure 3a, c, and d. Unlike the  $^{17}\text{O}$  MAS NMR spectra of dehydrated zeolite HY, in which the main signal from the framework sites is broad and featureless owing to the presence of similar concentrations

- (19) Larin, A. V.; Vercauteren, D. P. *J. Mol. Catal. A: Chem.* **2001**, *168*, 123–138.  
 (20) Xue, X.; Kanzaki, M. *J. Phys. Chem. B* **2001**, *105*, 3422–3434.  
 (21) Loeser, T.; Freude, D.; Mabande, G. T. P.; Schwieger, W. *Chem. Phys. Lett.* **2003**, *370*, 32–38.  
 (22) Stebbins, J. F.; Zhao, P. D.; Lee, S. K.; Cheng, X. *Am. Mineral.* **1999**, *84*, 1680–1684.  
 (23) Neuhoff, P. S.; Shao, P.; Stebbins, J. F. *Microporous Mesoporous Mat.* **2002**, *55*, 239–251.  
 (24) Kao, H. M.; Grey, C. P. *Chem. Phys. Lett.* **1996**, *259*, 459–464.  
 (25) Vega, A. J.; Luz, Z. *J. Phys. Chem.* **1987**, *91*, 365–373.  
 (26) Peng, L.; Liu, Y.; Kim, N.; Readman, J. E.; Grey, C. P. *Nat. Mater.* **2005**, *4*, 216–219.  
 (27) Czjzek, M.; Jobic, H.; Fitch, A. N.; Vogt, T. *J. Phys. Chem.* **1992**, *96*, 1535–1540.  
 (28) Redondo, A.; Hay, P. J. *J. Phys. Chem.* **1993**, *97*, 11754–11761.

- (29) Bak, M.; Rasmussen, J. T.; Nielsen, N. C. *J. Magn. Reson.* **2000**, *147*, 296–330.

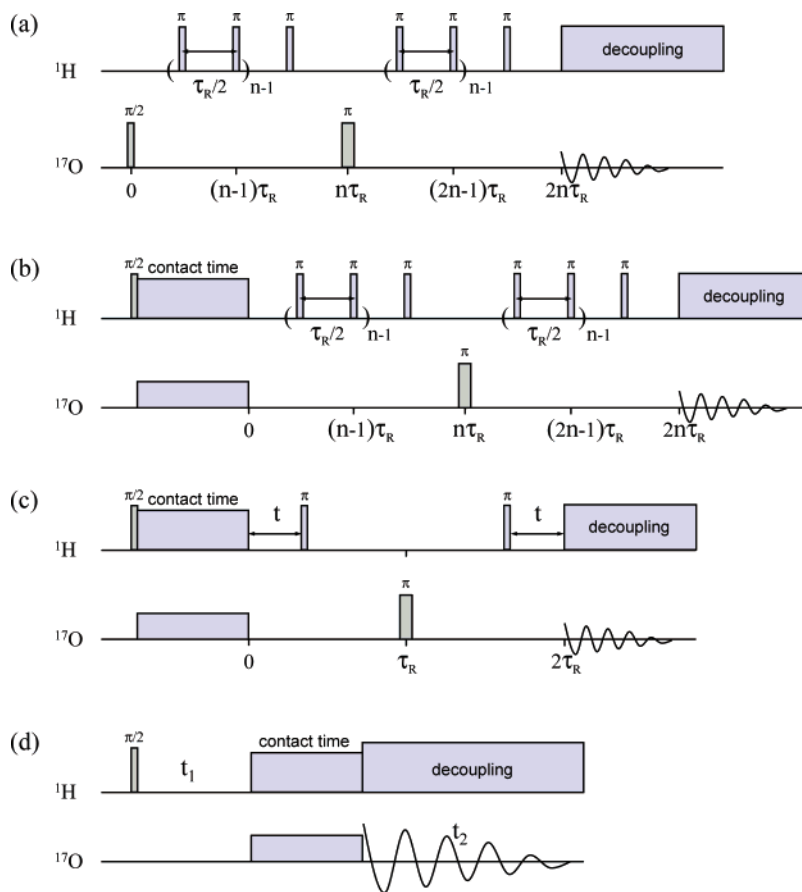


**Figure 2.** NMR pulse sequences. (a) <sup>17</sup>O-<sup>1</sup>H REDOR; (b) <sup>1</sup>H → <sup>17</sup>O CP-REDOR; (c) <sup>1</sup>H → <sup>17</sup>O-<sup>1</sup>H CP-REDOR with shifted  $\pi$  pulses; (d) 2-D <sup>1</sup>H-<sup>17</sup>O HETCOR NMR.

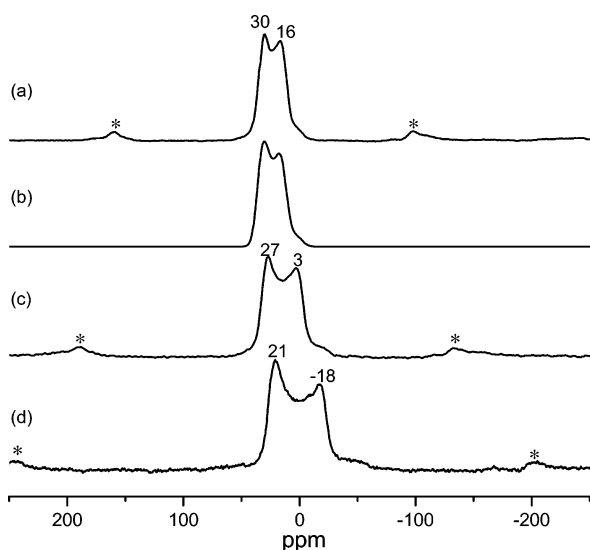


**Figure 3.** <sup>17</sup>O one-pulse spectra of <sup>17</sup>O-enriched HZSM-5 acquired at (a) 17.6, (c) 14.1, and (d) 11.7 T, with spinning speeds of 13, 13, and 15 kHz, respectively. Recycle delay: 1 s, Asterisks (\*) in this and subsequent spectra denote spinning sidebands. Short pulse lengths of 1.5–2.0  $\mu$ s were used, corresponding to  $\pi/8 \sim \pi/6$  pulses for  $H_2^{17}O$ . (b) <sup>17</sup>O MAS NMR simulation of the 17.6 T spectrum performed with the WSolids NMR package. Simulation parameters:  $\delta_{CS} = 40.5$ , QCC = 5.45 MHz, and  $\eta = 0.2$ .

of Si–O–Al and Si–O–Si linkages,<sup>26</sup> the resonance of HZSM-5 has a characteristic second-order quadrupolar line shape with clear discontinuities, mostly arising from the framework oxygen atoms in Si–O–Si environments. The

discontinuities shift to lower frequencies with decreasing magnetic field, which is consistent with the inverse dependence of the second-order quadrupolar interaction on the external field strength. A one-site simulation of the 17.6 T MAS NMR data is shown in Figure 3b, with  $\delta_{CS}$  (isotropic chemical shift) = 40.5 ppm, QCC (quadrupolar coupling constant) = 5.45 MHz, and  $\eta$  (asymmetry parameter) = 0.2; NMR simulations with these parameters also provide good fits to the lower-field data. These simulations provide an estimate for the average values of the NMR parameters of oxygen atoms in Si–O–Si linkages in dehydrated zeolite HZSM-5 and are similar to those found for Si–O–Si in other *hydrated* zeolites.<sup>11,17,18</sup>  $\delta_{CS}$  and  $\eta$  are similar to the values reported for hydrated NaZSM-5, while the value of QCC obtained in our study is slightly larger.<sup>18</sup>

A weak peak in the one-pulse <sup>17</sup>O MAS NMR spectra of zeolite HY, visible as a low frequency shoulder of the dominant framework resonance, was assigned in our previous work to oxygen atoms directly bound to Brønsted acid sites.<sup>26</sup> However, no clear shoulder is visible in the spectra of HZSM-5, even for spectra with very good signal/noise ratios. Thus, <sup>17</sup>O/<sup>1</sup>H double resonance NMR experiments were performed to search for the signals from the Brønsted acid sites.

**<sup>1</sup>H → <sup>17</sup>O CP-MAS NMR.** CP-MAS NMR spectroscopy has been shown to be helpful in investigating proximity between proton and oxygen nuclei.<sup>26,30</sup> The <sup>1</sup>H → <sup>17</sup>O CP-MAS spectra

(30) Brenn, U.; Ernst, H.; Freude, D.; Herrmann, R.; Jahnig, R.; Karge, H. G.; Karger, J.; König, T.; Madler, B.; Pingel, U. T.; Prochnow, D.; Schwieger, W. *Microporous Mesoporous Mater.* **2000**, *40*, 43–52.

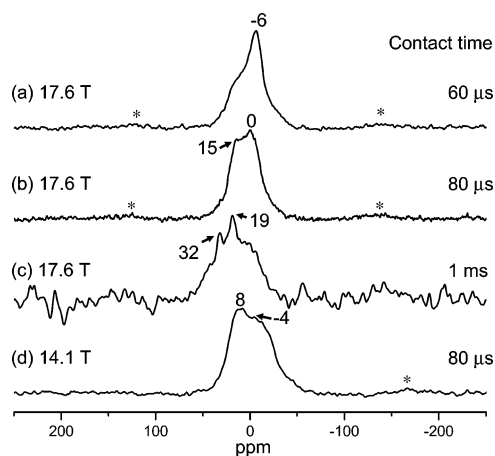


**Figure 4.**  $^1\text{H} \rightarrow ^{17}\text{O}$  CP-MAS NMR spectra of  $^{17}\text{O}$ -enriched zeolite HY (a) and HZSM-5 (b–d) acquired with different external field strengths and different contact times as indicated. Spinning speed, 13 kHz; recycle delay, 1 s.  $R_f$  field strengths of  $\omega_1(^{17}\text{O})/2\pi = 28$  kHz and  $\omega_1(^1\text{H})/2\pi = 91$  kHz were used. A total of 2048, 57732, 6400, and 143360 scans were used to collect the spectra shown in spectra a, b, c, and d, respectively.

of HY and HZSM-5 are shown in Figure 4a, b, and d. Short contact times were used to ensure that only resonances from the oxygen atoms bound to the Brønsted acid sites are observed. Compared to the one-pulse  $^{17}\text{O}$  NMR spectrum, the observed resonances are broader and the peak maxima have shifted to lower frequencies. While the CP resonance of HY (Figure 4a) has a line shape resembling that of a single quadrupolar site with a large asymmetry parameter ( $\eta \sim 1$ ), the line shape of the HZSM-5 resonance (Figure 4b and d) cannot be fit by using a simple one-site simulation. This suggests that there are a wider range of Brønsted oxygen atom environments in HZSM-5 than in HY. Primarily because of the much lower concentration of Brønsted acid sites in HZSM-5 than in HY, more than half a day of data collection was required to obtain a CP spectrum with good signal-to-noise (S/N) for HZSM-5, while only half an hour was required for HY; the HY sample could even be used to set the Hartmann–Hahn condition for CP.

The CP intensity was measured as a function of contact time (Figure 5). The contact time corresponding to the maximum CP signal is  $60 \mu\text{s}$  for zeolite HY, this value increasing to  $80 \mu\text{s}$  for zeolite HZSM-5. A slower CP build up curve for zeolite HZSM-5 may indicate a longer O–H distance in HZSM-5 than in HY or some residual motion of the O–H group. However, the CP dynamics of quadrupolar nuclei can be very complicated and the contact time value for the CP maximum may depend on many factors including not only the cross-polarization time  $T_{IS}$ , but also  $T_{1\rho}^{\text{H}}$  and  $T_{1\rho}^{\text{O}}$ , the relaxation times in the rotating frame for  $^1\text{H}$  and  $^{17}\text{O}$ , respectively.<sup>31–33</sup> In particular, the ability to maintain the  $^{17}\text{O}$  spin-locking depends sensitively on the MAS frequency and the quadrupolar coupling parameters.<sup>34,35</sup>

Figure 4c shows CP-MAS spectrum of HZSM-5 with a contact time of 1 ms at 17.6 T. With longer contact times, in addition to the overall signal loss, resonances due to oxygen atoms not directly bound to the acidic protons are also excited

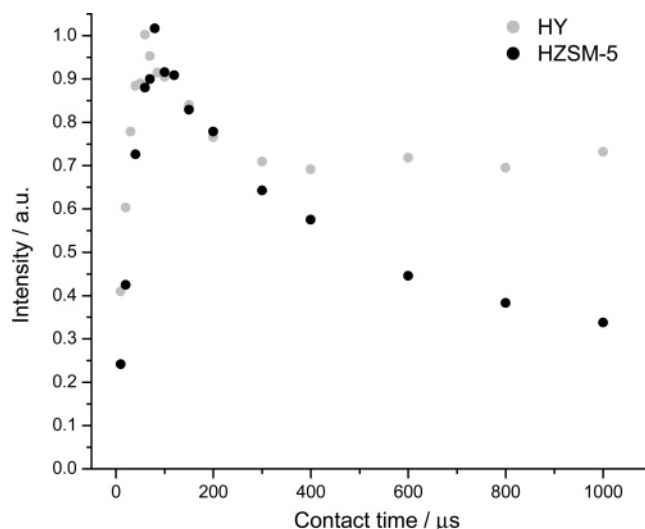


**Figure 5.** Plot of the signal intensity obtained in the  $^1\text{H} \rightarrow ^{17}\text{O}$  CP-MAS spectrum of zeolites HY and HZSM-5 at 17.6 T as a function of contact time: spinning speed, 13 kHz; recycle delay, 1 s.

and an increased concentration of oxygen atoms in Si–O–Si linkages, which resonate at positive frequencies, are observed (Figure 4b).

**$2\text{-D}^1\text{H}\text{-}^{17}\text{O}$  HETCOR NMR.** Most zeolite structures contain more than one possible location for the Brønsted acid proton. Furthermore, the  $^1\text{H} \rightarrow ^{17}\text{O}$  CP-MAS NMR spectrum of HZSM-5 cannot be fit with a single set of NMR parameters, suggesting that the local environments for the Brønsted acid sites may be quite different. Thus methods are required to separate the  $^{17}\text{O}$  resonances associated with the various Brønsted acid sites. The different Brønsted acid sites can sometimes be resolved in their  $^1\text{H}$  MAS NMR spectrum, which is the case for zeolite HY.<sup>13,36–41</sup> Thus,  $^1\text{H}\text{-}^{17}\text{O}$  HETCOR experiments were performed in order to correlate specific  $^1\text{H}$  resonances with their corresponding  $^{17}\text{O}$  signals, by making use of the strong dipolar coupling between the  $^{17}\text{O}$  and  $^1\text{H}$  nuclei.

The spectrum of HY obtained at 17.6 T is shown in Figure 6a. The projection of the  $^1\text{H}$  dimension clearly shows two resonances at 3.7 and 4.4 ppm from the Brønsted acid sites in the supercages and sodalite cages,<sup>13,36–41</sup> respectively (Figure 1). The  $^{17}\text{O}$  signals corresponding to these sites can be identified by extracting slices along the  $^{17}\text{O}$  dimension taken at the appropriate  $^1\text{H}$  frequencies (Figure 6b–e). The two sets of  $^{17}\text{O}$  NMR parameters obtained from simulations of these two slices are only slightly different from each other and are consistent with our  $^{17}\text{O}$  MQMAS results.<sup>42</sup> Compared to the parameters reported in our earlier Communication and obtained by using the  $^{17}\text{O}\text{-}^1\text{H}$  REDOR NMR method, where the spectra were fit by making the assumption that there is only one oxygen site (Table 1),<sup>26</sup> the values of asymmetry parameters obtained in the 2D HETCOR experiment are slightly larger, while the

(31) Kolodziejewski, W.; Klinowski, J. *Chem. Rev.* **2002**, *102*, 613–628.  
 (32) Mehring, M. *Principles of High Resolution NMR in Solids*; Springer-Verlag: Berlin, Heidelberg, New York, 1983.  
 (33) Pines, A.; Gibby, M. G.; Waugh, J. S. *J. Chem. Phys.* **1973**, *59*, 569–590.  
 (34) Vega, A. J. *J. Magn. Reson.* **1992**, *96*, 50–68.  
 (35) Vega, A. J. *Solid State Nucl. Magn. Reson.* **1992**, *1*, 17–32.

(36) Hunger, M. *Solid State Nucl. Magn. Reson.* **1996**, *6*, 1–29.  
 (37) Ernst, H.; Freude, D.; Wolf, I. *Chem. Phys. Lett.* **1993**, *212*, 588–596.  
 (38) Freude, D.; Hunger, M.; Pfeifer, H.; Schwiager, W. *Chem. Phys. Lett.* **1986**, *128*, 62–66.  
 (39) Freude, D.; Klinowski, J.; Hamdan, H. *Chem. Phys. Lett.* **1988**, *149*, 355–362.  
 (40) Freude, D.; Ernst, H.; Wolf, I. *Solid State Nucl. Magn. Reson.* **1994**, *3*, 271–286.  
 (41) Grey, C. P.; Vega, A. J. *J. Am. Chem. Soc.* **1995**, *117*, 8232–8242.  
 (42) Peng, L. Ph.D. Dissertation, State University of New York at Stony Brook, 2006.



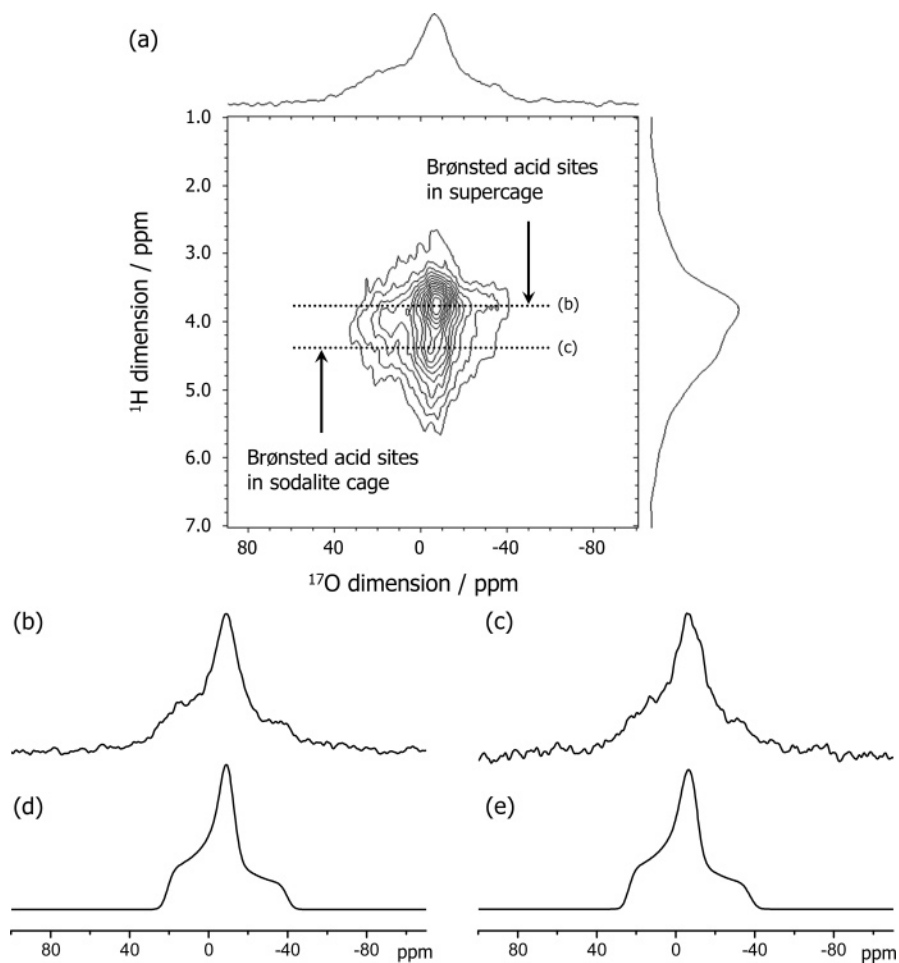


**Figure 6.** (a) 2-D <sup>1</sup>H-<sup>17</sup>O HETCOR NMR spectrum of zeolite HY obtained at 17.6 T. Contact time = 80 μs; spinning speed = 13 kHz; recycle delay = 1 s. A total of 64 and 1024 points were acquired in the first and second dimensions, respectively, with 4800 scans per time increment, so that the full 2D spectrum took 3 days + 14 h to acquire. Slices and simulations of the <sup>17</sup>O dimension corresponding to the Brønsted acid site in the supercage (b and d) and sodalite cage (c and e) are shown. Simulation parameters are shown in Table 1. The dashed lines in the 2-D spectra show where the slices were taken.

**Table 1.** Comparison of the NMR Parameters of <sup>17</sup>O Atoms Directly Bound to Brønsted Acid Sites in Zeolite HY Obtained from the Simulations of the HECTOR NMR Slices with Those Obtained Earlier from One-Pulse and REDOR NMR Data<sup>26</sup>

	$\delta_{CS}$	QCC/ MHz	$\eta$
Brønsted acid sites in supercage $\delta_{CS} (^1\text{H}) = 3.7$	21(1)	6.0(1)	1.0(1)
Brønsted acid sites in sodalite cage $\delta_{CS} (^1\text{H}) = 4.4$	24(1)	6.2(1)	0.9(1)
Brønsted acid sites: Earlier REDOR data <sup>26</sup>	28(1)	6.6(1)	0.8(1)

quadrupolar coupling constants are smaller, than the values extracted from the 1D REDOR experiment. The errors in our earlier measurement are ascribed to the small, but significant difference in the values of  $\delta_{iso}$ , between the two sites, which resulted in an error in our determination of the QCC.

<sup>1</sup>H MAS NMR spectrum of zeolite HZSM-5 is shown in Figure 7a. The dominant signal due to Brønsted acid sites is at 4.2 ppm. However, there is a broader component at a slightly more positive chemical shift, indicative of different Brønsted acid site environments. A deconvolution of this resonance is shown in Figure 7b,c. At least two different resonances at approximately 4.6 and 4.8 ppm appear to be buried under the main Brønsted acid signal. The broader signal at higher frequencies (approximately 7 ppm) has been assigned to residual

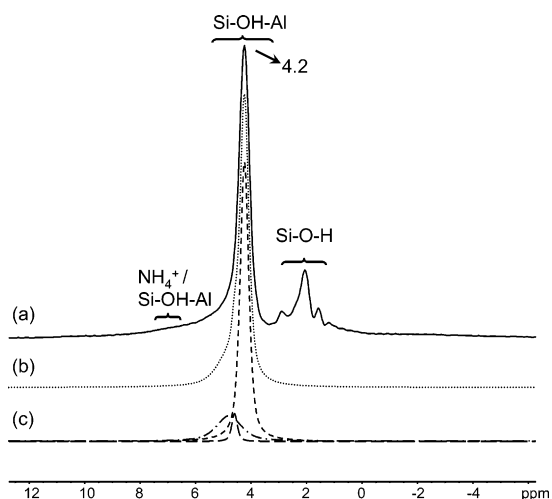


**Figure 7.** <sup>1</sup>H spin-echo MAS NMR spectra of zeolite HZSM-5. (a) Experimental spectrum acquired with a spinning speed of 13 kHz and recycle delay of 2 s. The resonance at approximately 4.2 ppm was deconvoluted with 3 resonances at 4.2, 4.6, and 4.8 ppm (c) and the sum is shown in spectra b.

NH<sub>4</sub><sup>+</sup> groups that also resonate in this frequency range<sup>13,37,39</sup> and/or an additional Brønsted acid site.<sup>43,44</sup>

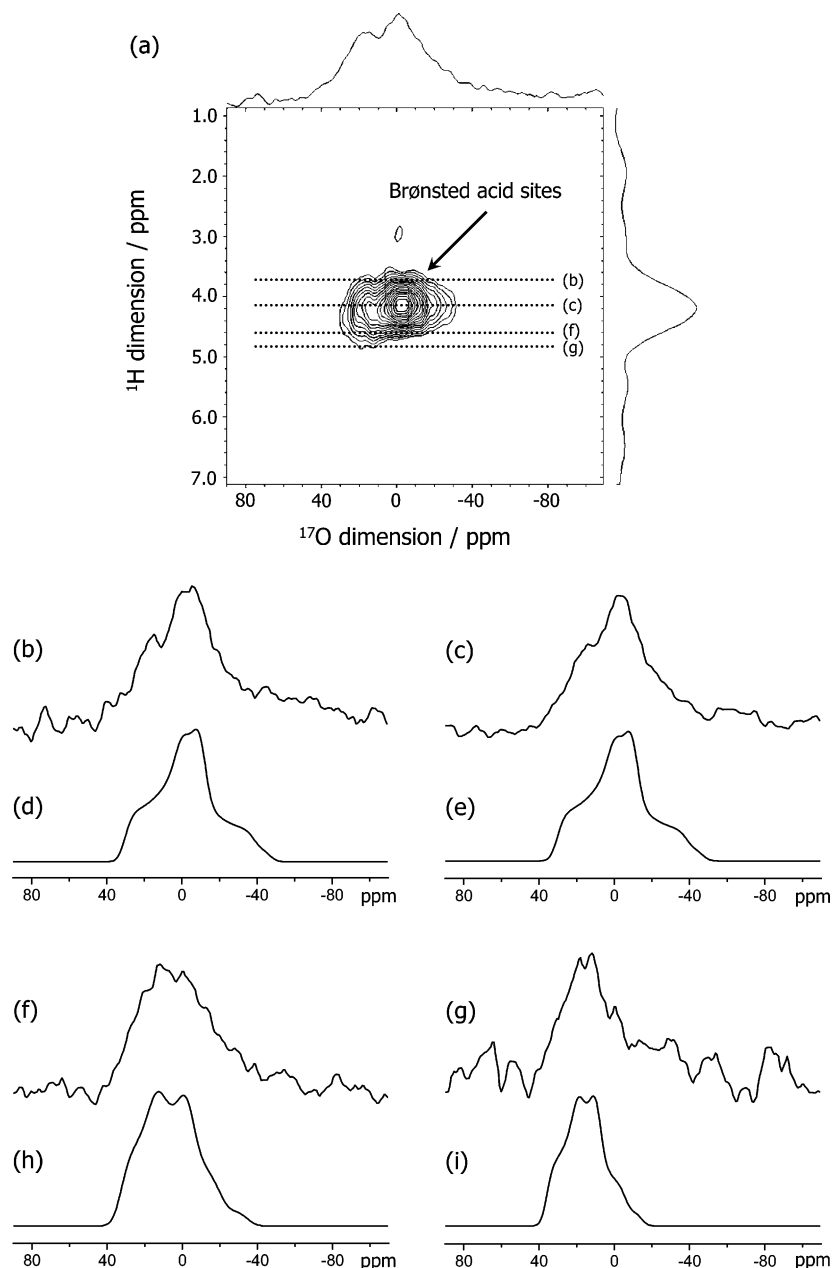


**Figure 8.** (a) 2-D  $^1\text{H}$ - $^{17}\text{O}$  HETCOR NMR spectrum of zeolite HZSM-5 obtained at 17.6 T. Contact time = 80  $\mu\text{s}$ ; spinning speed = 13 kHz, recycle delay = 1 s. A total of 38 and 1024 points were acquired in the first and second dimensions, respectively, with 10800 scans per time increment, i.e., 4 days + 18 h acquisition time. (b, c, f, g) Slices of the  $^{17}\text{O}$  dimension at  $\delta_{\text{CS}}(^1\text{H}) = 3.7, 4.2, 4.6,$  and  $4.8$  in the 2-D HETCOR NMR spectrum, respectively. (d, e, h, i) Simulation of Brønsted acid site at  $\delta_{\text{CS}}(^1\text{H}) = 3.7, 4.2, 4.6,$  and  $4.8$ , respectively. The parameters used in these simulations are given in Table 2. The dotted lines in the 2-D spectra show where the slices are taken.

The 2-D  $^1\text{H}$ - $^{17}\text{O}$  HETCOR NMR spectrum of zeolite HZSM-5 is shown in Figure 8a. Although only one main resonance is observed, which connects Brønsted acidic protons and oxygen atoms, the slices at different  $^1\text{H}$  chemical shifts are quite different. The  $^{17}\text{O}$  line shapes were simulated and the NMR parameters were obtained (Figure 8b–i). Slices taken at more negative  $^1\text{H}$  shifts (Figure 8b) have very similar line shapes compared to the slices taken at the center ( $\delta_{\text{CS}}(^1\text{H}) = 4.2$ , Figure 8c), and these slices can be simulated with same NMR parameters. Although the slices obtained at more positive  $^1\text{H}$  shifts (Figure 8f,g) are associated with poor S/N, they cannot

be simulated satisfactorily with the same parameters as used for the 4.2 ppm slice, and the  $^{17}\text{O}$  sites connected to these protons are clearly associated with quite different quadrupolar and chemical shift parameters. Furthermore, the HETCOR data confirm that there are additional  $^1\text{H}$  resonances due to different proton sites hidden under the main 4.2 ppm Brønsted acid site resonance. Estimates for the quadrupolar and chemical shift parameters of these sites are included in Table 2, and despite the poor S/N of the spectra and the consequent errors in the determination of these values, there appears to be a noticeable decrease in the QCC between these sites and those of the main HZSM-5 site, the decrease being more pronounced for the site associated with the 4.8 ppm  $^1\text{H}$  resonance. Simulations of the “4.6” and “4.8” ppm oxygen sites with different QCCs and

(43) Beck, L. W.; White, J. L.; Haw, J. F. *J. Am. Chem. Soc.* **1994**, *116*, 9657–9661.

(44) Freude, D. *Chem. Phys. Lett.* **1995**, *235*, 69–75.

**Table 2.** NMR Parameters of <sup>17</sup>O Atoms Directly Bound to Brønsted Acid Sites in Zeolite HZSM-5 Obtained from Simulations of the HETCOR NMR Slices

	$\delta_{CS}$	QCC / MHz	$\eta$
Brønsted acid sites ( $\delta_{CS}$ ( <sup>1</sup> H) = 4.2)	31(2)	7.0(2)	0.75(20)
Brønsted acid sites ( $\delta_{CS}$ ( <sup>1</sup> H) = 4.6)	35(2)	6.8(4)	0.5(2)
Brønsted acid sites ( $\delta_{CS}$ ( <sup>1</sup> H) = 4.8)	37(2)	5.8(6)	0.6(3)

values of  $\eta$  are provided in the Supporting Information, to illustrate the errors associated with the simulations, particularly in the determination of  $\eta$  (Figure S1). Since the HETCOR spectrum took almost 5 days to obtain, it was not feasible to acquire data with improved S/N.

Shifts to higher frequencies in the <sup>1</sup>H NMR of zeolites have been ascribed to either more acidic sites or to sites that are more strongly hydrogen-bonded to other framework oxygen sites. The sites in the supercages of HY (Figure 1) are believed to be more acidic than those in the sodalite cages.<sup>38,45,46</sup> Thus, the latter explanation is generally used to rationalize the more positive shifts observed for the Brønsted acid sites located in the smaller (sodalite) cages of HY, since these sites are likely associated with shorter H–O<sub>framework</sub> distances than those of the supercage sites.<sup>36,47,48</sup> On this basis, the resonance at 4.2 ppm in HZSM-5 is assigned to the Brønsted acid protons in the main channel of HZSM-5 (Figure 1), while the resonances at 4.6/4.8 ppm are tentatively assigned to environments within the channels that are more strongly hydrogen-bonded to other framework sites or to sites within the small pentasil cages. Further experiments are in progress to confirm these assignments. Although the broad peak at approximately 7 ppm has been assigned to a Brønsted acid site,<sup>43,44</sup> we were not able to detect the <sup>17</sup>O signal associated with this site, possibly because of either the breadth of the <sup>1</sup>H signal or motion of the protons that give rise to this signal. Consistent with this latter suggestion, a noticeable sharpening of this <sup>1</sup>H resonance was observed by Beck et al. on cooling a sample of HZSM-5 to 123 K, suggesting that the protons that give rise to this resonance are mobile at room temperature.<sup>43</sup> Difficulties in detecting this weak resonance may also arise from the low-frequency oscillations in the second dimension of the HETCOR NMR spectrum because of the limited number of *t*<sub>2</sub> points used in the experiment.

**<sup>1</sup>H → <sup>17</sup>O-<sup>1</sup>H CP-REDOR NMR.** CP-REDOR NMR, developed by Gullion and Schaefer,<sup>49</sup> has become a standard solid-state NMR technique for measuring heteronuclear distances under MAS conditions. Our initial <sup>17</sup>O-<sup>1</sup>H REDOR experiments, reported previously for HY,<sup>26</sup> used a simple short pulse to excite the <sup>17</sup>O spins (Figure 2a). This REDOR sequence allowed for a ready separation of the framework and Brønsted acid sites, for both zeolites HY<sup>26</sup> and HZSM-5, the Brønsted acid sites being clearly observed in the so-called difference spectrum (the difference between the control and the double resonance spectra). The framework and Brønsted acid sites, however, have quite different spin–spin relaxation times, *T*<sub>2</sub>; thus, accurate measurements of the REDOR fractions, (1 –

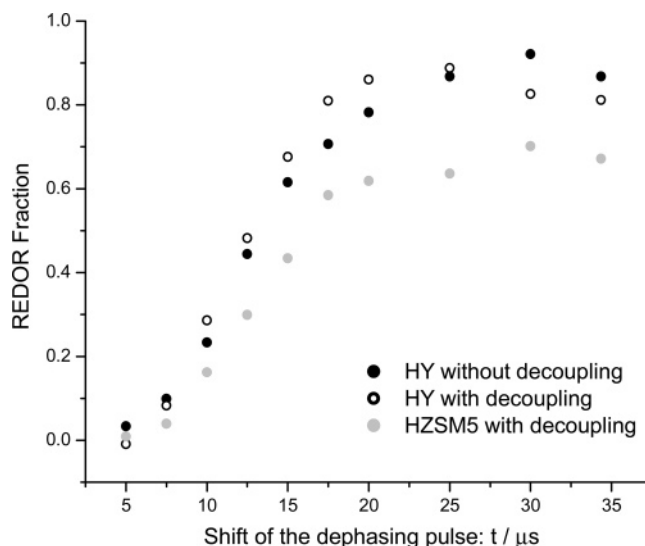


**Figure 9.** <sup>1</sup>H → <sup>17</sup>O-<sup>1</sup>H CP-REDOR NMR fraction (1 – *S*/*S*<sub>0</sub>) measured as a function of the shift of the first dephasing pulse (time, *t*; see Figure 2c) with (HY and HZSM-5) and without (HY) <sup>1</sup>H decoupling during the acquisition period. Spinning speed, 13 kHz; recycle delay, 1 s; field strength, 17.6 T; <sup>1</sup>H  $\pi$  pulse, 6.2  $\mu$ s.

*S*/*S*<sub>0</sub>), where *S*<sub>0</sub> and *S* are obtained by integrating the signals in the control and double resonance spectra, are extremely prone to error for strongly overlapping sites, particularly when the site of interest is extremely weak in intensity, relative to the dominant (framework) site: *S*<sub>0</sub> will contain varying contributions from the two groups of sites as a function of the dephasing time, 2*n* $\pi$  $\tau$ . Hence, all the experiments reported here made use of a CP excitation sequence. Because of the very large <sup>1</sup>H-<sup>17</sup>O dipolar coupling for O–H groups, a “mirror-symmetric” pulse sequence (Figure 2c) was used<sup>50–52</sup> rather than the pulse sequence often used for quadrupolar nuclei<sup>49,53</sup> shown in Figure 2b.

The REDOR fractions were measured as a function of time *t*, which represents the time between the end of the contact time and the <sup>1</sup>H  $\pi$  pulse, that is, the shift of the pulse (Figure 2c). The *t* = 1/2 rotor period (i.e., 34.3  $\mu$ s for a spinning speed of 13 kHz) corresponds to the maximum evolution time for the <sup>17</sup>O spins, under the influence of the <sup>1</sup>H dipolar coupling. Data were acquired without the two dephasing  $\pi$  pulses, which were used as the control experiments. Two data sets, with and without <sup>1</sup>H decoupling, during the acquisition period, were acquired to investigate the effect of <sup>1</sup>H-<sup>17</sup>O dipolar coupling on different parts of the <sup>17</sup>O line shape. Owing to the signal-to-noise limitations of the experiment, the REDOR fractions were measured by integrating the isotropic resonances only, and not the sidebands, and the CP-REDOR fractions of zeolites HY and HZSM-5 are shown in Figure 9. The REDOR fractions increase with increasing value of time *t* and reach a maximum when *t* is approximately 25 and 30  $\mu$ s, for the data with and without decoupling, respectively. The REDOR fractions are noticeably smaller for HZSM-5 than for HY, and do not reach 100%, even at the maximum dephasing times used in both experiments. The

(45) Hoffmann, J.; Hunger, B.; Streller, U.; Stock, T.; Dombrowski, D.; Barth, A. *Zeolites* **1985**, *5*, 31–36.  
 (46) Jacobs, W. P. J. H.; Jobic, H.; Vanwolput, J. H. M. C.; Vansanten, R. A. *Zeolites* **1992**, *12*, 315–319.  
 (47) Freude, D.; Hunger, M.; Pfeifer, H. *Z. Phys. Chem. (NF)* **1987**, *152*, 171–182.  
 (48) Hunger, M.; Anderson, M. W.; Ojo, A.; Pfeifer, H. *Microporous Mater.* **1993**, *1*, 17–32.  
 (49) Gullion, T.; Schaefer, J. *J. Magn. Reson.* **1989**, *81*, 196–200.

(50) Goetz, J. M.; Wu, J. H.; Yee, H. F.; Schaefer, J. *Solid State Nucl. Magn. Reson.* **1998**, *12*, 87–95.  
 (51) Gullion, T. *Magn. Reson. Rev.* **1997**, *17*, 83–131.  
 (52) Wu, J. H.; Xiao, C. D.; Yee, A. F.; Goetz, J. M.; Schaefer, J. *Macromolecules* **2000**, *33*, 6849–6852.  
 (53) Fyfe, C. A.; Mueller, K. T.; Grondy, H.; Wong-Moon, K. C. *J. Phys. Chem.* **1993**, *97*, 13484–13495.

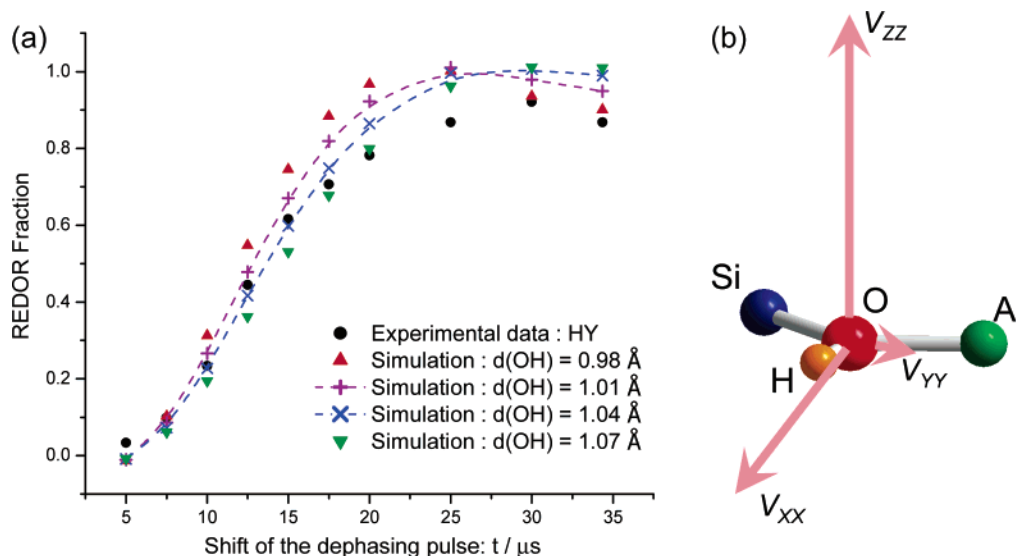


**Figure 10.** (a) Comparison of experimental  $^1\text{H} \rightarrow ^{17}\text{O}$  REDOR fractions with those obtained by using the SIMPSON package. Dipolar coupling constants of 17308, 15811, 14482, and 13298 Hz were used in simulations, corresponding to O–H distances of 0.98, 1.01, 1.04, and 1.07 Å, respectively. NMR parameters used are  $\delta_{\text{CS}} = 21$ ,  $\text{QCC} = 6.0$  MHz, and  $\eta = 1$ . No  $^1\text{H}$  decoupling was applied in the experiments and simulations. (b) The orientation of the principal axis of the electric field gradient (EFG), defined by  $V_{ZZ}$ ,  $V_{XX}$ , and  $V_{YY}$  with respect to the Si–O(H)–Al group, used in the simulations. This orientation was obtained from our ab-initio calculations reported earlier<sup>26</sup> (see Supporting Information (Figure S2) and the main text).

more rapid dephasing observed for HY, for the dataset acquired with  $^1\text{H}$  decoupling, is consistent with the large  $^{17}\text{O}$ – $^1\text{H}$  dipolar coupling in this system; sidebands are present in the non- $^1\text{H}$  decoupled spectra, which will originate from parts of the powder with larger than average dipolar couplings; the centerband will, therefore, contain parts of the powder with a smaller effective dipolar coupling constant. This effect is analyzed in more detail later.

Numerical simulations with typical O–H distances are compared with the experimental REDOR fractions of zeolite HY in Figure 10a. All these simulations were performed by calculating the  $^{17}\text{O}$  spectrum obtained following a REDOR dephasing sequence. The centerband was then integrated allowing comparison with the REDOR fractions extracted from the experimental data. The Euler angles used in the simulation, which define the relative orientations between the principal axis system (PAS) of the dipolar and quadrupolar tensors with respect to the crystal fixed frame, were obtained from our ab-initio calculations, reported earlier.<sup>26</sup> The orientation of the EFG PAS with respect to the  $\text{O}_1$  Brønsted acid site, obtained from ab-initio calculations is shown in Figure 10b:  $V_{ZZ}$  is aligned perpendicular to the Si–O–Al plane,  $V_{YY}$  is in the Si–O–Al plane, while  $V_{XX}$  deviates only slightly (by  $13^\circ$ ) from the O–H direction (Figure S2). Further details concerning the simulations can be found in the Supporting Information. The calculated data qualitatively fit the experimental data, the oscillation in the calculated curve occurring at a similar dephasing time as the experimental data for an O–H distance of 1.04 Å. The initial rise of the experimental REDOR fraction curve is closer to that seen in the calculated 1.01–1.04 Å curves. However, unlike the calculated curves, the experimental maximum REDOR fraction does not reach 1.0.

A closer inspection of the experimental CP-REDOR line shape, as a function of the dephasing time, indicates that the dephasing is not constant for the whole second-order quadrupolar line shape. The intensity (at approximately 8 ppm, at 17.6 T) in between the high-frequency discontinuity (at approximately

18 ppm) and the middle, most intense frequency discontinuity (at about  $-7$  ppm) drops the most rapidly and becomes negative when the dephasing time  $t$  is about  $25\sim 30 \mu\text{s}$  and then becomes positive again when  $t$  increases above  $30 \mu\text{s}$ . The main discontinuity, and the intensity to lower frequencies, decreases with increasing  $t$ , but remains positive at all dephasing times. The differences in the dephasing behavior across the line shapes reflect the fact that the various components of the second-order line shape arise from different parts of the powder and, thus, are associated with different effective dipolar coupling constants. A similar effect has been previously observed in the  $^{17}\text{O}$ – $^{31}\text{P}$  REDOR spectra of phosphate glasses<sup>54</sup> and in the  $^1\text{H}$ – $^{17}\text{O}$  CP buildup curves of brucite ( $\text{Mg}(\text{OH})_2$ ) and  $\text{Mg}(\text{OH})_{2-x}(\text{OCH}_3)_x$ .<sup>55</sup>

The line shapes of the CP-REDOR NMR spectra of HY (acquired without  $^1\text{H}$  decoupling) were simulated (Figure 11) as a function of the O–H distance. The fit between the experimental and simulated spectra with 0.98–1.01 Å is surprisingly good; for example, the frequency of the oscillation of the signal at around 8 ppm is very similar in both the experimental and calculated data. However, the major discontinuity at  $-7$  ppm reaches a minimum at approximately  $17.5\text{--}20.0 \mu\text{s}$ , while no clear oscillation is observed experimentally. The change of the intensities of the sidebands were also extremely sensitive to small changes in the dipolar coupling constant, since faster oscillations are seen in the sideband than in the centerband, with best fits being obtained with distances of between 0.98 and 1.01 Å.

Simulations confirmed that the change in the second-order quadrupolar line shape with dephasing time is strongly affected by the relative orientation between the dipolar and quadrupolar tensors (Figure 12), in principle providing a method for determining the relative orientations between the two tensors, as demonstrated previously in the earlier  $^{17}\text{O}$ – $^{31}\text{P}$  REDOR study.<sup>54</sup> Simulations were, therefore, performed to validate the

(54) Zeyer, M.; Montagne, L.; Jaeger, C. *Solid State Nucl. Magn. Reson.* **2003**, *23*, 136–144.

(55) van Eck, E. R. H.; Smith, M. E. *J. Chem. Phys.* **1998**, *108*, 5904–5912.



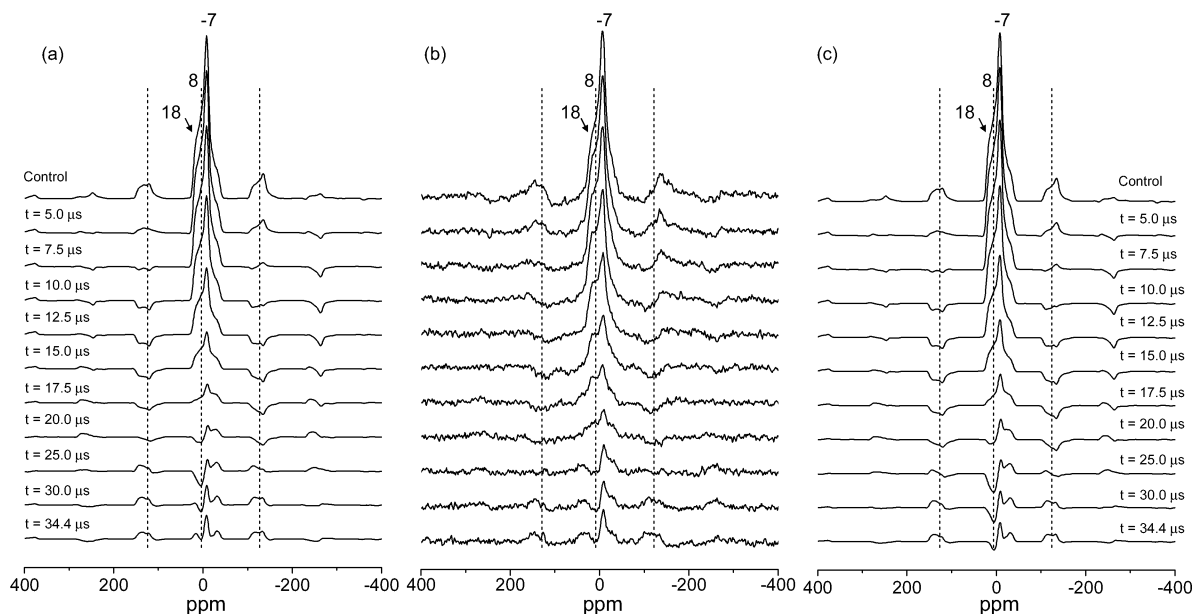


**Figure 11.** (b) Experimental <sup>1</sup>H → <sup>17</sup>O-<sup>1</sup>H CP-REDOR NMR spectra, acquired without <sup>1</sup>H decoupling, as a function of the shift of the first dephasing pulse (time, *t*) at 17.6 T and (a, c) simulations performed with dipolar coupling constants corresponding to O–H distances of 0.98 and 1.01 Å, respectively, and no <sup>1</sup>H decoupling. NMR parameters used are  $\delta_{CS} = 21$ , QCC = 6.0 MHz, and  $\eta = 1$ . Further simulations with different O–H distances can be found in the Supporting Information (Figure S7).

relative orientations of the dipolar and EFG tensors obtained in the ab-initio calculations. Rotations of the PAS that defines the EFG tensor, so that principal axes of the new PAS (described by  $V_{ZZ}'$ ,  $V_{XX}'$ , and  $V_{YY}'$ ) lie along one of the original PAS directions, generally result in significant differences in the REDOR dephasing spectra (see, for example, Figure 12c,d, where  $V_{YY}'$  is aligned along  $V_{XX}$  (the OH direction) and  $V_{YY}'$  is aligned perpendicular to the Si–O–Al plane, respectively). However, when  $V_{XX}'$  is aligned along  $V_{ZZ}$  and  $V_{ZZ}'$  is aligned along  $V_{XX}$  (data not shown), no change is observed, presumably because  $|V_{XX}| = |V_{ZZ}|$ , when  $\eta = 1$ , and thus no effect is expected on interchanging these axes. The line-shape changes seen in the simulations performed with  $V_{YY}'$  aligned along the O–H direction are very different from those seen experimentally, while the simulations obtained with  $V_{YY}'$  perpendicular to the Si–O–Al plane (and  $V_{ZZ}'$  approximately along the O–H direction) provide a better fit to the data, but not quite as good as the fit with  $V_{YY}$  in the Si–O–Al plane (and  $V_{XX}$  along O–H), although given the S/N of the spectra it is not possible to rule out this orientation of the PAS. Thus, the REDOR data support the EFG tensor orientations obtained from the ab-initio calculations and indicate that one of the two largest components of the EFG tensor ( $V_{ZZ}$  or  $V_{XX}$ ) must lie very close to the O–H direction. Even small changes in the relative orientations of the two tensors result in noticeable changes in the spectra, as illustrated in the simulations provided in the Supporting Information (Figures S3–S4), confirming the sensitivity of these spectra to the EFG PAS. It is important to note that the REDOR fractions ( $1 - S/S_0$ ) are not sensitive to the relative orientation of the quadrupolar and dipolar tensors, as expected (Figure S6).

The simulations of REDOR fractions of HZSM-5 were also performed (not shown). Again, based on the time taken to reach the maximum in the REDOR fraction, the ( $1/r^3$ -weighted) average O–H distance in zeolite HZSM-5 was estimated to be 1.10 Å. Unfortunately, because of a distribution of different local environments in zeolite HZSM-5 and the consequent distribution

in NMR parameters, and the poorer S/N of these experiments, a simulation of the CP-REDOR line shape was not straightforward and was not attempted. The noticeably smaller REDOR fractions for HZSM-5 in comparison to those of HY for all values of *t* (Figure 9) can be ascribed to either a longer O–H distance or increased mobility, or a combination of both. The presence of higher mobility in HZSM-5 is consistent with <sup>1</sup>H MAS NMR studies on both these zeolites.<sup>56</sup> The effect of motion on the spectra is explored in the next section.

**<sup>17</sup>O Variable-Temperature MAS NMR of HY.** To explore any possible proton motion, variable temperature <sup>17</sup>O MAS NMR spectra were acquired for zeolite HY at 14.1 T. A comparison of the <sup>17</sup>O one-pulse MAS NMR spectra of HY at 173 and 293 K is shown in Figure 13. The Brønsted acid site resonance at approximately –24 ppm<sup>26</sup> has a much more distinct second-order quadrupolar line shape with sharper discontinuities at the lower temperature. In addition, the most intense discontinuity shifts from –24 to –26 ppm at low temperature. The high-temperature <sup>17</sup>O spin-echo MAS NMR spectra acquired at 11.7 T are shown in Figure 14 for comparison. The resonance due to Brønsted acid sites at –45 ppm broadens and appears to decrease in intensity with increasing temperature. At 498 K, this peak almost completely disappears, presumably as a result of proton motion. All of these observations indicate the presence of some residual proton motion at room temperature, even in HY. At room temperature this motion is likely caused by vibrations of the zeolite framework and librations of the O–H groups, while at higher temperatures, proton hops between sites can occur.<sup>56,57</sup> These proton hops are thought to involve jumps between the four oxygen atoms bound to a central Al atom.<sup>56,57</sup> Slower motion will initially result in a broadening of the Si–O(H)–Al and Si–O–Al resonances, but when the motion is

(56) Sarv, P.; Tuherm, T.; Lippmaa, E.; Keskinen, K.; Root, A. *J. Phys. Chem.* **1995**, *99*, 13763–13768.

(57) Freude, D.; Oehme, W.; Schmiede, H.; Staudte, B. *J. Catal.* **1974**, *32*, 137–143.

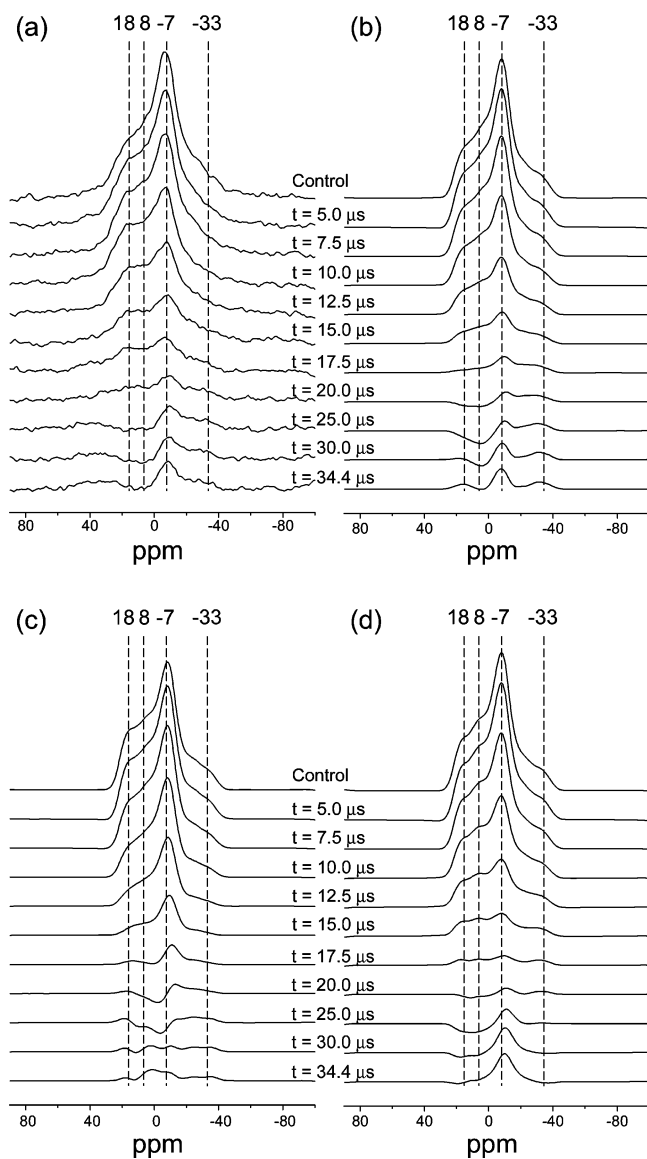


**Figure 12.** Comparison of experimental and calculated  $^1\text{H} \rightarrow ^{17}\text{O}$  REDOR NMR spectra. (a) experimental data. The simulations with the PAS of the quadrupolar tensor defined by (b)  $V_{ZZ}$  perpendicular to the Si–O–Al plane,  $V_{XX} = 13.7^\circ$  from the O–H direction,  $V_{YY}$  in the Si–O–Al plane (as shown in Figure 10b); (c)  $V_{XX}$  perpendicular to the Si–O–Al plane,  $V_{YY} = 13.7^\circ$  from the O–H direction; (d)  $V_{YY}$  perpendicular to the Si–O–Al plane,  $V_{ZZ} = 13.7^\circ$  from the O–H direction. Simulations were performed with an O–H distance of 0.98 Å. Spinning speed = 13 kHz;  $\delta_{CS} = 21$ , QCC = 6.0 MHz, and  $\eta = 1$ ; no  $^1\text{H}$  decoupling.

rapid on a time scale controlled by the separation in frequencies between these two resonances, coalescence of the Si–O–Al and Si–O(H)–Al resonances will occur, resulting in a resonance with a chemical shift intermediate between those of the two resonances, the exact value of the shift depending on whether all four O atoms are equally involved in this process. The centers of gravity for the Si–O–Al resonances may be estimated from the one-pulse spectra, or obtained with more accuracy from the MQMAS spectra.<sup>42</sup> At a field strength of 11.7 T, the difference between the centers of gravities of these two resonances is approximately 4 kHz, and thus motion with a frequency approaching this value is expected to broaden the resonances. Although this represents only a crude estimate of the time scale of motion, it is consistent with the estimates for motion made on the basis of  $^1\text{H}$  MAS NMR data at high temperature, where

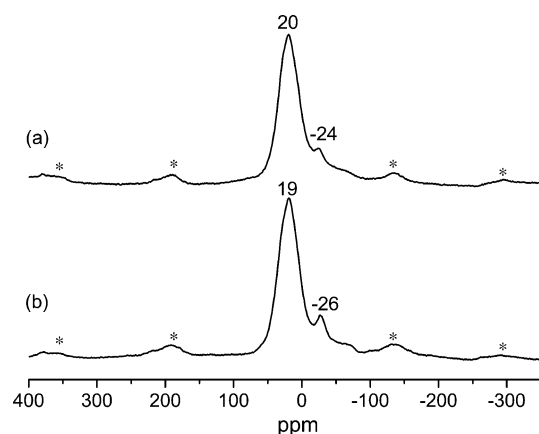


**Figure 13.** 14.1 T  $^{17}\text{O}$  MAS NMR of zeolite HY at (a) 293 and (b) 173 K: spinning speed, 13 kHz; recycle delay, 1 s.

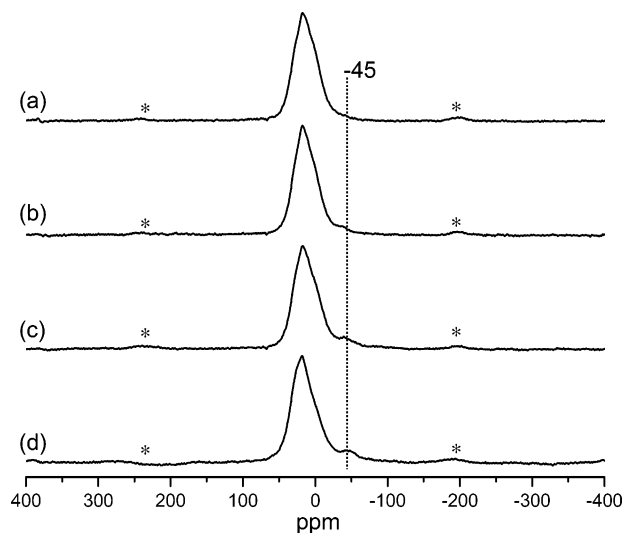


**Figure 14.** 11.7 T  $^{17}\text{O}$  spin-echo MAS NMR of zeolite HY at (a) 498, (b) 423, (c) 348, and (d) 298 K: spinning speed, 15 kHz; recycle delay, 1 s.

a rough estimate for the hop frequency of approximately 2.2 kHz or higher was obtained at above 568 K.<sup>56</sup> A more detailed analysis of these spectra should include an analysis of the effect of the motion on the reorientation of the quadrupolar tensors and the consequent effect of this on the averaging of the second-order quadrupolar line shape, as performed, for example, by Farnan et al.<sup>58</sup> and Schurko et al.,<sup>59</sup> for exchange between the same crystallographic sites, and between sites, which is the case here, by Kotecha et al.,<sup>60</sup> but is beyond the scope of this paper. Similar experiments have not been attempted at this time for HZSM-5, since the Brønsted acid site resonance cannot be readily discerned in the one-pulse spectra.

**The Effect of Motion on the Internuclear Distances.** The distance extracted from the REDOR line-shape simulations (0.98–1.01 Å) is shorter than the value obtained from the best fit to the REDOR fraction curve (1.04 Å) but is still slightly longer than the O–H distances obtained from ab-initio calculations of Brønsted acid sites (0.97–0.98 Å).<sup>19,20,61</sup> Clearly, something is not captured in our simulations of the REDOR

(58) Kristensen, J. H.; Farnan, I. *J. Chem. Phys.* **2001**, *114*, 9608–9624.

(59) Schurko, R. W.; Wi, S.; Frydman, L. *J. Phys. Chem. A* **2002**, *106*, 51–62.

(60) Kotecha, M.; Chaudhuri, S.; Grey, C. P.; Frydman, L. *J. Am. Chem. Soc.* **2005**, *127*, 16701–16712.

(61) Fois, E.; Gamba, A.; Tabacchi, G. *J. Phys. Chem. B* **1998**, *102*, 3974–3979.

line shapes, which results in a reduction of the extent of dephasing of certain parts of the line shape, and thus smaller apparent REDOR fractions for the whole powder. The variable temperature  $^{17}\text{O}$  NMR spectra suggest that the most likely explanation for this is the presence of restricted motion, in principle involving proton hops between different framework sites,<sup>56</sup> or librational motion of the O–H group and of the framework itself; although this motion will result in an apparent reduction in the average dipolar coupling, it will also affect the various components of the line shape differently. Librational motion of the zeolite framework itself may be quite large even at ambient temperatures and is responsible for phenomena such as the negative thermal expansion that has been seen for some zeolites.<sup>62</sup> The variable temperature NMR suggest that proton hopping is significant, particularly at elevated temperatures.

Librational motion and bond stretches occur at time scales that are much shorter than the NMR time scale, and will result in averaging of the dipolar coupling tensor, and thus longer apparent distances. This motion has been analyzed in detail by Ishii et al. for glycine, who showed that the effect of libration was much more significant for atoms directly bound to hydrogen.<sup>63</sup> For example, the N–H and C–H distances measured at room temperature by NMR were between 3.7 and 5.3% longer than the “correct” distances, where the correct distances were defined as the distances between the time-averaged values of the two atoms obtained in their molecular dynamics simulations. These differences are consistent with the differences between the values measured here by REDOR NMR line shape simulations (0.98–1.01 Å) and those obtained earlier from ab-initio methods. O–H distances have also been measured by symmetry-based recoupling sequences, and longer apparent distances have similarly been measured at room temperature in these experiments. For example, Brinkmann et al.<sup>64</sup> measured a distance of 1.04 Å for the O–H bond in  $^{17}\text{O}^{\eta}$ -L-tyrosine, which was noticeably larger than the distance measured by diffraction, 0.989 Å. Van Beek et al. obtained an O–H distance in brucite  $\text{Mg}(\text{OH})_2$  that was much longer (12.6%) than the value obtained by diffraction, by using a different recoupling scheme (PRESTO),<sup>65</sup> but the reason for this large difference was unclear. Ishii et al. pointed out that the librational motion will also result in a dipolar tensor that is no longer axially symmetric; this will also result in a difference between the calculated spectra and REDOR curves, and experimental data.<sup>63</sup> More simulations are in progress to explore this phenomenon. The longer range, much slower, proton motion is also expected to partially average the O–H dipolar coupling and this motion may also help explain why the REDOR fractions do not reach their theoretical maxima. While this motion will be frozen out at lower temperatures, even at 0 K discrepancies between NMR and “correct” O–H distances of approximately 2–3% are expected because of zero-point librational motion.

**Structural Implications.** According to the neutron diffraction data for HY,<sup>27</sup> the oxygen atoms directly bound to Brønsted acid sites have quite distinct O–H distances: very short O–H distances are observed for oxygen atoms pointing into the

supercage ( $\text{O}_1\text{--H}_1 = 0.82$  Å), while longer distances are observed for oxygen atoms pointing into the sodalite cage ( $\text{O}_2\text{--H}_2 = 1.02$  and  $\text{O}_3\text{--H}_3 = 0.98$  Å). Concentrations for  $\text{O}_1/\text{O}_2/\text{O}_3$  of 54:18:28% were found for these sites.<sup>27</sup> The O–H length determined for the predominant site ( $\text{O}_1$ ) is noticeably shorter than the O–H distances extracted from the simulations, while the  $\text{O}_2\text{--H}_2$  and  $\text{O}_3\text{--H}_3$  distances are closer to those seen experimentally by NMR, particularly when the effect of motion is accounted for. We note, however, that a distance of 0.82 Å is not physically reasonable and must result from errors associated with the refinements of structures containing disorder. The O–H distance determined by diffraction represents a distance between the proton position and the average location for O in a Si–O–Si or Si–O–Al linkage; given that the two linkages are associated with quite different bond-angles, local structural distortions of the framework are likely and these will not necessarily be captured in the average structure obtained in the refinements.

The O–H $\cdots$ O bond lengths of many model compounds have been investigated by using X-ray/neutron diffraction, and correlations exist between the O–H distance and the O $\cdots$ O distance, when the O $\cdots$ O distance drops below 2.70 Å (the strong hydrogen-bonding regime).<sup>66–68</sup> However, when the O $\cdots$ O distance is longer than 2.70 Å (the weak hydrogen-bonding regime) the bond length changes are typically small and an O–H distance of 0.95–1.00 Å is generally observed.<sup>66–68</sup> Little or only weak H-bonding is expected for HY, again consistent with the experimental estimates of the O–H distances of between 0.98 and 1.01 Å. Our results are also consistent with the ab-initio calculations which give an O–H length of 0.984 Å for the Si–OH–Al environment in hydrogen sodalite;<sup>61</sup> similar or slightly shorter distances have been obtained in other ab-initio calculations.<sup>19,20,69–71</sup> Thus, the O–H distances measured for HY are consistent with both experimental and calculated data for O–H groups. However, further work is clearly needed to (I) to account for the motion observed in these systems, and (II) develop methods for measuring O–H distances for the different Brønsted acid sites.

The QCCs of the oxygen atoms directly bound to the Brønsted acid site (Si–O(H)–Al) are noticeably larger than the experimentally determined values of the oxygen atoms in Si–O–Al or Si–O–Si linkages, in both zeolites HY and HZSM-5,<sup>14,16–18,21,23,30</sup> indicating that the oxygen bonding environment at the Brønsted acid site is quite different and more distorted than the normal framework site. The asymmetry parameters ( $\eta$ ) are large ( $\geq 0.5$ ), consistent with a large distortion of the oxygen environment from axial symmetry. The QCCs and values of  $\eta$  are in reasonable agreement with those obtained from ab-initio calculations, where QCCs of 6.5 to 8.8 MHz<sup>19,20,26</sup> and values of  $\eta$  of 0.8–1.0 are typically observed. The experimental QCCs, particularly those of HY, are lower than the calculated values (for example, values of 6.5–7.9 MHz were obtained for clusters resembling fragments of HY).<sup>26</sup> Similar discrepancies have been observed for oxygen atoms in Si–OH groups, where the

(62) Lightfoot, P.; Woodcock, D. A.; Maple, M. J.; Villaescusa, L. A.; Wright, P. A. *J. Mater. Chem.* **2001**, *11*, 212–216.

(63) Ishii, Y.; Terao, T.; Hayashi, S. *J. Chem. Phys.* **1997**, *107*, 2760–2774.

(64) Brinkmann, A.; Kentgens, A. P. M. *J. Phys. Chem. B* **2006**, *110*, 16089–16101.

(65) van Beek, J. D.; Dupree, R.; Levitt, M. H. *J. Magn. Reson.* **2006**, *179*, 38–48.

(66) Ichikawa, M. *Acta Crystallogr., Sect. B: Struct. Sci.* **1978**, *34*, 2074–2080.

(67) Ichikawa, M. *J. Mol. Struct.* **2000**, *552*, 63–70.

(68) Joswig, W.; Fuess, H.; Ferraris, G. *Acta Crystallogr., Sect. B: Struct. Sci.* **1982**, *38*, 2798–2801.

(69) Eichler, U.; Brandle, M.; Sauer, J. *J. Phys. Chem. B* **1997**, *101*, 10035–10050.

(70) Haase, F.; Sauer, J. *J. Am. Chem. Soc.* **1995**, *117*, 3780–3789.

(71) Schroder, K. P.; Sauer, J. *J. Phys. Chem.* **1996**, *100*, 11043–11049.

experimentally determined QCCs are much smaller than the calculated ones.<sup>30,72</sup> Note that none of the zeolite calculations were performed with periodic boundary conditions, and it may be that the clusters used in the calculations are too flexible (or too small). The QCCs can also be quite sensitive to the basis sets used in the ab-initio calculations, which must also account for some of the differences between the values obtained in the various calculations and the experimental values.

Sites in the supercages of HY ( $O_1-H$ )<sup>27</sup> (Figure 1) are associated with only a slightly larger value of  $\eta$  and a slightly smaller QCC than those in the sodalite cages ( $O_2-H$  and  $O_3-H$ ). These sites bridge two 4-rings (and the 12-ring in the supercage) ( $O_1$ ), two 4-rings and one 6-ring ( $O_3$ ), and one 4-ring and two 6-rings ( $O_2$ ), and so the similarity in the quadrupolar parameters is not too surprising. Quite different quadrupolar parameters and chemical shifts are observed for the main proton site coordinated to the five-membered rings that make up the pentasil units of HZSM-5; this site is located in the HZSM-5 channels. Generally, Si-O-X bond angles in pentasil units are slightly larger ( $153-169^\circ$ )<sup>73</sup> than those seen in faujasites ( $135.7-144.6^\circ$ ),<sup>27</sup> which may account for the differences in NMR parameters, although differences in the flexibilities of the framework, Si/Al ratios, and O...O H-bonding distances may also be important. In both HY and HZSM-5, sites with larger  $^1H$  chemical shifts are associated with larger  $^{17}O$  chemical shifts, although there does not appear to be a clear trend between the changes in the QCC and  $\eta$  and the chemical shift. For example, in HZSM-5, the sites that are associated with larger  $^1H$  shifts are thought to be located inside the pentasil units and consequently more strongly H-bonded to other nearby oxygen atoms. This appears to result in a noticeable decrease in QCC. No such trend is observed for the sodalite vs supercage protons, where the increase in  $^1H$  chemical shift for the sodalite protons has similarly been ascribed to stronger H-bonding. Clearly experimental data from a wider range of zeolites is required in order to develop more systematic trends between the  $^{17}O$  NMR and structural parameters.

## Conclusions

The  $^{17}O$ , one-pulse NMR spectra of H-form zeolites are dominated by the signals due to the framework Si-O-Si and Si-O-Al sites. In the case of the low Si/Al ratio zeolite HY, a weaker  $^{17}O$  NMR signal can also be detected from the Brønsted acid site, while for the high Si/Al ratio zeolite HZSM-5, this site could not be clearly resolved in this study, even at very high fields. However, the large  $^{17}O-^1H$  dipolar coupling ( $>15$  kHz) between the Brønsted acid oxygen framework site and the Brønsted acid proton could be exploited to select the  $^{17}O$  Brønsted acid signal, in both  $^1H \rightarrow ^{17}O$  CP and  $^{17}O-^1H$  REDOR experiments. These 1D experiments revealed that the acid sites in HZSM-5 are associated with a wide range of NMR parameters, while those for HY are similar. This observation

was confirmed by performing  $^1H-^{17}O$  2D-HETCOR NMR experiments, in which the  $^1H$  signals were connected to their respective  $^{17}O$  signals. Two different oxygen sites were resolved for HY with QCCs of 6.0 and 6.2 MHz, corresponding to oxygen atoms pointing into the super- and sodalite cages, respectively. In contrast, the main channel sites in HZSM-5 zeolite are associated with a much larger QCC (7.0 MHz), while the more strongly H-bonded sites in the channels or inside the pentasil units are associated with smaller QCCs.

A mirror-symmetric  $^{17}O-^1H$  REDOR pulse sequence was employed in order to measure the very short O-H bond lengths present in these systems. The REDOR dephasing curves appear to be affected by residual motion complicating the analysis of the experimental data. Nonetheless, simulations of the REDOR fractions and changes in the second-order line shape with dephasing time suggest a bond length of between 0.98–1.01 Å for HY, which is typical of an O-H group with no or only weak H-bonding. These distances are noticeably longer than the distance measured for the major HY O site in a previous neutron diffraction experiment; the unreasonably short distance seen in the diffraction experiment is ascribed to the presence of local distortions around the Brønsted acid site that are not captured in this long-range probe of structure. HZSM-5 appears to be associated with longer O-H bond lengths and/or increased motion than HY, both suggestions being consistent with the stronger acidity expected for this system. The second-order quadrupolar lineshapes in the REDOR spectra are also very sensitive to the relative orientations of the dipolar and quadrupolar PAS; simulations indicate that the largest values of the EFG tensor are located along the O-H direction. Variable temperature  $^{17}O$  NMR spectra confirmed the presence of proton motion in HY and indicated the presence of framework vibrations and/or O-H librations, even at room temperature.

The work opens up new methods for investigating local structure in acid zeolites and for investigating the local structural changes that occur in the vicinity of the Brønsted acid site that are not readily captured in a diffraction experiment. The results suggest quite different local environments for the Brønsted acid sites in the two zeolites studied in this work. Work on a wider range of zeolite frameworks and with varying Si/Al ratios is currently in progress to develop more detailed correlations between NMR parameters, structural parameters and acidity.

**Acknowledgment.** We thank Drs. Martine Ziliox and Boris Itin for their help in obtaining the 14.1 and 17.6 T NMR data. Financial support was provided by the DOE via Grant DEFG0296ER14681; we thank the NSF for a grant to purchase the 11.7 T instrument (Grant CHE 0321001). The 17.6 T NMR resources at New York Structural Biology Center (NYSBC) are supported by NIH P41 GM66354.

**Supporting Information Available:** Additional simulation results. This material is available free of charge via the Internet at <http://pubs.acs.org>.

JA064922Z

(72) Xue, X.; Kanzaki, M. *Phys. Chem. Miner.* **1998**, *26*, 14–30.

(73) Vankoningsveld, H.; Jansen, J. C.; Vanbekkum, H. *Zeolites* **1990**, *10*, 235–242.